INSTITUTE OF PHYSICS PUBLISHING JOURNAL OF PHYSICS D: APPLIED PHYSICS

J. Phys. D: Appl. Phys. **39** (2006) R151–R161 doi:10.1088/0022-3727/39/8/R01

TOPICAL REVIEW

Magnetophotonic crystals

M Inoue[1,2,3], R Fujikawa[1], A Baryshev[1], A Khanikaev[1], P B Lim[2], H Uchida[1], O Aktsipetrov[3], A Fedyanin[3], T Murzina[3] and A Granovsky[3]

[1]Toyohashi University of Technology, Toyohashi, Aichi 441-8580, Japan
[2]CREST, Japan Science and Technology Agency, Saitama 332-0012, Japan
[3]Lomonosov Moscow State University, Leninskie Gory, Moscow, 119992, Russian Federation

E-mail: inoue_mitsuteru@eee.tut.ac.jp

Received 22 November 2005
Published 30 March 2006
Online at stacks.iop.org/JPhysD/39/R151

Abstract

When the constitutive materials of photonic crystals (PCs) are magnetic, or even only a defect introduced in PCs is magnetic, the resultant PCs exhibit very unique optical and magneto-optical properties. The strong photon confinement in the vicinity of magnetic defects results in large enhancement in linear and nonlinear magneto-optical responses of the media. Novel functions, such as band Faraday effect, magnetic super-prism effect and non-reciprocal or magnetically controllable photonic band structure, are predicted to occur theoretically. All the unique features of the media arise from the existence of magnetization in media, and hence they are called magnetophotonic crystals providing the spin-dependent nature in PCs.

(Some figures in this article are in colour only in the electronic version)

1. Introduction

In much the same way that semiconductor crystals affect the propagation of electrons, photonic crystals (PCs) (periodic composites of macroscopic dielectric media of different refractive index) affect the propagation of light, providing a new mechanism to control and manipulate the flow of light. The key to this lies in the concept of a photonic bandgap originating in the periodic structure itself and localization of light in the vicinity of defects introduced into the periodic structure [1].

When the constitutive material of PCs is magnetic, or even only a defect introduced into the periodic structure is magnetic, the resultant PCs (let us simply refer to them as magnetophotonic crystals (MPCs) hereafter) exhibit unique optical and magneto-optical responses. The strong photon confinement associated with the magnetic defect can be exploited to enhance and optimize magneto-optical (MO) effects and optical nonlinearity of existing materials. In fact, large enhancement in MO Faraday and Kerr effects have been demonstrated with one-dimensional (1D) MPCs composed of a magnetic garnet thin film sandwiched between dielectric Bragg mirrors [2, 3]. The enhancement in MO Faraday response can be also seen at the edges of the photonic bandgap appearing in $(Bi:YIG/SiO_2)^n$ multilayer films [4]. The large MO enhancement is particularly attractive for constructing film-type optical isolator/circulator elements as theoretically predicted in [5] for optical communication systems and ultra-high-speed MO spatial light modulators for high density holographic data storage as examined in [6] experimentally.

Strong enhancement in resonant second-harmonic generation (SHG) intensity was also obtained for the 1D-MPCs within the spectral range of the pass band. Both significant nonlinear MO Kerr effect (NOMOKE) rotation of second-harmonic wave polarization and magnetization-induced variations of the SHG intensity (MSHG) were detected in the vicinity of a localized photonic state. The spectral asymmetry (non-reciprocity) is also expected to occur in MPCs with proper spatial arrangement of magnetic and dielectric components [8], which has never been observed in conventional non-magnetic PCs. Strictly speaking, these studies with transparent 1D-MPCs are considered to be those of reflection MSHG as a consequence of the Faraday effect. Traditionally, however, experiments in the reflection geometry are named in magneto-optics as Kerr effects.

Ordered pore array structures have been examined as templates for two-dimensional (2D) MPCs. A good candidate

for this is a porous alumina (Al_2O_3) plate with an almost perfect periodic hole structure. They are actually employed in the 2D-MPC formation as a mask in physical etching of the Bi:YIG film [9] or as a container template of the sol–gel Bi:YIG precursor solution. Quite recently, the selective-area epitaxial growth of the magnetic garnet films has been studied for MPC formation. Within a considerably large area, beautiful 1D or 2D periodic magnetic domain patterns were demonstrated suggesting the usefulness of the method [10]. These 2D MPCs are expected to be useful for constructing programmable optical circuit devices [78]. According to theoretical investigations, spin-dependent photonic band structures and magnetically controllable superprism effects are both expected to occur in such 2D-MPCs and the following 3D- MPCs [11].

An artificial opal (3D PCs composed of dielectric fine particles) can be a template for the 3D-MPCs, where magnetically active materials fill up the free periodic space within the opal [12]. In fact, 3D-MPCs thus prepared exhibit unique MO wavelength spectra originating in the existence of the photonic band gap structure [71, 73]. Introduction of a magnetically active point, line or plane defects into the 3D periodic structure is also interesting, because such a defect can support the localized modes of light within the 3D structure, and the linear and nonlinear enhanced MO effect associated with the localized light is expected.

In this paper, based upon our recent studies on magnetophotonic crystals, their preparation and unique properties are reviewed in detail.

2. Magneto-optical responses of layered media

A series of our MPC studies dates back to 1995, where the light propagation in discontinuous magnetic media with a 1D array structure was discussed [13]. In subsequent theoretical studies [14–17], light propagation in bismuth-substituted yttrium iron garnet (Bi:YIG) films with random multilayer structures was analysed using the matrix approach [18], where unique enhancement of the MO effects associated with the localization of light were predicted. To see this situation, as shown in figure 1, let us consider a multilayer film composed of N_M layers of Bi:YIG and N_S layers of SiO_2 which are piled up in an arbitrary sequence. Each Bi:YIG and SiO_2 layers has a thickness of d_M and d_S, respectively, and the total thickness of the multilayer film is D. The density of Bi:YIG in the film, P_M, is then defined by $P_M = N_M d_M/D$. For simplicity, all Bi:YIG (SiO_2) films are assumed to have the same material parameters.

Figure 2 is a typical example of transmissivity T, Faraday rotation angle θ_F and total rotation angle $\theta = \theta_F N_M d_M$ of films for λ wavelength of light) = 1.15 μm is depicted as a function of the Bi:YIG density P_M. The film is composed of 16 layers with the structure of 1010101110101010, where '1' denotes the Bi:YIG film while '0' the SiO_2 film. As marked by arrows in figure 2, films with (1) $P_M = 0.09$, (2) 0.123, (3) 0.291 and (4) 0.668 show high transmissivity T and large θ_F simultaneously: for instance, T of the film with $P_M = 0.123$ is 91% and its θ_F is about four times larger than that of the Bi:YIG single-layer film ($\theta_F = -0.1^\circ\,\mu m^{-1}$ at $\lambda = 1.15\,\mu$m). The unique enhancements in both transmissivity and Faraday rotation

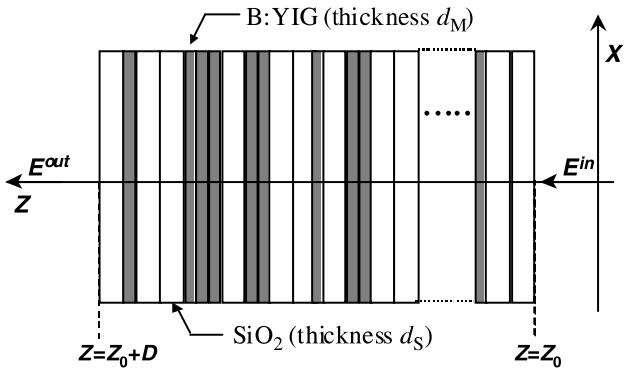

Figure 1. A layered medium with magnetic garnet films and silicon dioxide films which were stacked in an arbitrary sequence.

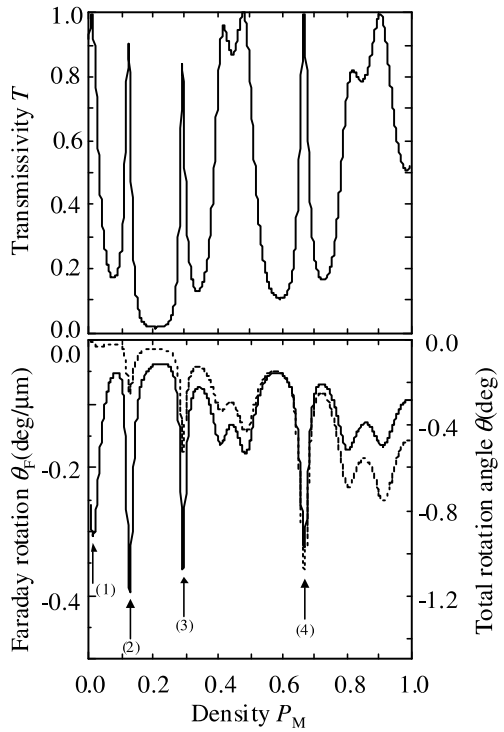

Figure 2. Transmissivity T, Faraday rotation angle θ_F (——), and total rotation angle $\theta = \theta_F N_M d_M$ (- - - -) versus Bi:YIG density $P_M = N_M d_M/D$ of the 16-layer film at $\lambda = 1.15\,\mu$m.

originate from the weak localization of light (or enhanced back scattering observed in disordered systems [59,60]) caused by the multiple interference. These results indicate that the enhancement in θ_F becomes larger when the degree of light localization is high: In fact, our theoretical computation showed the large enhancement in θ_F can be obtained in the 1D-MPCs with microcavity structures [20] with a magnetic defect was introduced into the periodic structure.

Figure 3 shows a typical example of the wavelength spectra of T and θ_F for such a film. The multilayer film was designed under the condition of $n_M d_M = n_S d_S = \lambda/4$ ($\lambda = 1.15\,\mu$m) with refraction indices n_M and n_S of the Bi:YIG and SiO_2 films, respectively. Note that the thickness of the central Bi:YIG film is different from other Bi:YIG layers and is regarded as a magnetic defect which breaks the periodic structure. The film provides a resonant transmission of light at

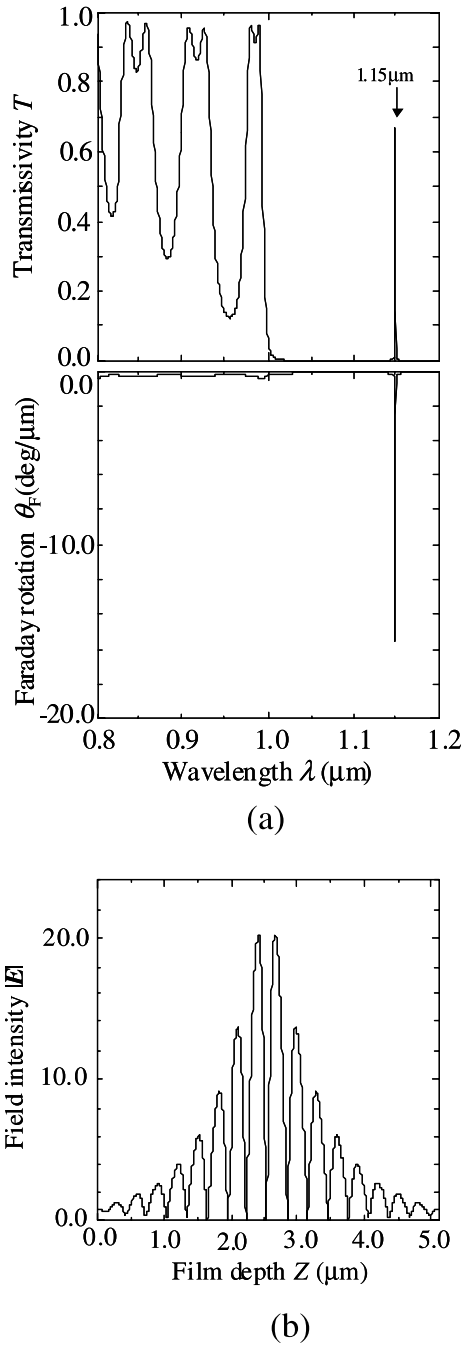

Figure 3. (*a*) Wavelength spectra of transmissivity T and Faraday rotation angle θ_F of the multilayer with $(Bi{:}YIG/SiO_2)_8/Bi{:}YIG_2/(SiO_2/Bi{:}YIG)_8$ structure, (*b*) electrical field distribution of light at $\lambda = 1.15\,\mu$m corresponding to the localization of light.

$\lambda = 1.15\,\mu$m with a large Faraday rotation of $-16^\circ\,\mu m^{-1}$. In comparison with the case of weak localization of light shown in figure 2, light is strongly localized within the film, yielding the huge enhancement in the Faraday effect. Such a film with a Bragg mirror sandwich is now called a magnetophotonic microcavity, which supports strongly localized modes of light within a photonic bandgap originating from the Fabry–Perot resonation. The performance of magnetic Fabry–Perot resonators, or bulk-type magnetic cavities was discussed by Rosenberg *et al* in 1964 [77] and Gomi *et al* in 1983 [61]. The magnetophotonic microcavity is then regarded as an extension of the bulk type of 1D film type, but its concept including the expansion to 2D or 3D artificial structures lies before us more importantly as novel magneto-optic media with spin-dependent photonic bandgap structures and localized modes of light.

The large enhancement in MO effects described above is explained in terms of the circular birefringence, as a result of the different localization conditions (localization wavelengths, for instance) for left- and right-hand circularly polarized lights possessing slightly different propagation velocities (refractive indices) to each other [20]. Smart explanation of the enhancement in θ_F due to the localization of light has also been given by Levy *et al* [19], where they discussed the performance of films with multi-microcavity structures exhibiting very large Faraday rotation without reducing the transmissivity being attractive for optical isolator applications. Further detailed theoretical discussions including the magneto-optical quality factor for localized modes and at band edges of 1D-MPCs can be found in [21–23] for both Faraday and Kerr operations.

3. 1D magnetophotonic crystals

3.1. Preparation of media and their linear properties

The theoretical predictions described in 2 were confirmed experimentally by forming two types of film samples: one had the microcavity structure of $(Ta_2O_5/SiO_2)^5/Bi{:}YIG/(SiO_2/Ta_2O_5)^5$ [3], while the other had the periodic structure of $(SiO_2/Bi{:}YIG)^5/Bi{:}YIG$ [4]. Both samples were prepared on Corning #1737 glass substrates with a conventional RF magnetron sputtering apparatus. Each Bi:YIG film was annealed immediately after its deposition by removing the sample from the vacuum chamber, where rapid thermal annealing at 700 °C for 15 min. was employed so as to avoid the growth of Bi:YIG grains. According to XRD and MO measurements of films, the annealing conditions were satisfactory to obtain a $Bi_{0.7}Y_{2.3}Fe_5O_{12}$ single garnet-phase polycrystalline film.

as shown in figures 4(*a*) and (*b*), 1D-MPCs with the Bi:YIG films had good layered structures, whose interfaces are well defined. The thickness of each film was as follows: Bi:YIG: 167 nm, SiO_2: 111 nm and Ta_2O_5: 92 nm for the microcavity structure, and Bi:YIG: 98 nm and SiO_2: 147 nm for the periodic alternative structure. In the preparations, the samples were post-annealed after every deposition of Bi:YIG films.

In figure 5, transmittance T (%) and rotation angle θ (deg) of the 1D-magnetophotonic microcavity are shown as a function of the wavelength of light which was submerged perpendicularly into the film plane. The MO response was measured under the Faraday geometry with a magnetic field of 7 kOe, the value of which was sufficient for magnetization saturation of Bi:YIG. In the figure, the solid curves are theoretical values calculated with the matrix approach [19], while open and closed marks denote the observed values in the magnetophotonic microcavity and a 167 nm-thick Bi:YIG single layer film, respectively. Within a photonic bandgap between 600 and 850 nm, resonant transmission of light due to the localization occurred at 720 nm, where the transmittance T=63% and the rotation angle $\theta = -0.63^\circ$

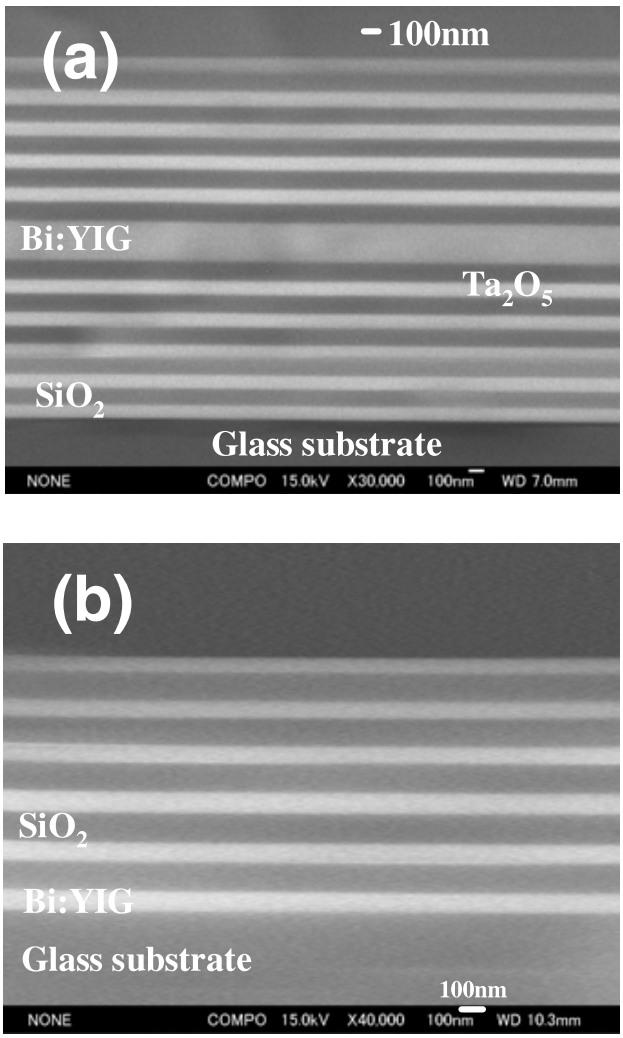

Figure 4. Cross-sectional SEM images of the 1D-MPCs: (*a*) microcavity structure of $(Ta_2O_5/SiO_2)_5$/Bi:YIG/$(SiO_2/Ta_2O_5)_5$ and (*b*) periodic structure of $(Bi:YIG/SiO_2)_5$/Bi:YIG.

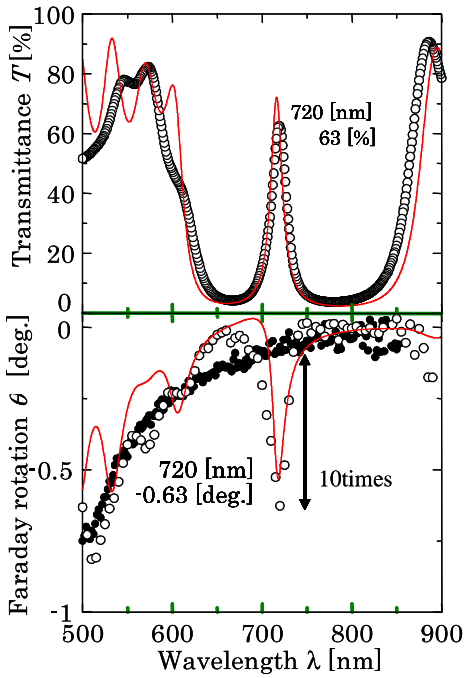

Figure 5. Wavelength spectra of transmittance T (top) and rotation angle θ (bottom) of the 1D-magnetophotonic microcavity shown in figure 4(*a*).

were obtained. Good quantitative agreement between the observed and calculated values is seen, suggesting that the magnetophotonic microcavity provides high transmissivity and large enhancement in θ simultaneously, which is very useful for various magnetophotonic applications.

Another important feature of the microcavity is its controllability in optical and magneto-optical responses of media. As demonstrated in figure 6, by controlling the thickness of the central Bi:YIG layer, the localization wavelength can be modified continuously and widely within the photonic bandgap. This enables us to design the media so as to be suitable for particular applications, in spite of the fact that a material design which meets the requirements is generally very tough. The media controllability remains in a wide range of wavelengths of light, unless the interference of light diminishes due to optical absorption.

In figure 7, wavelength spectra of transmissivity and rotation angle of the film with $(SiO_2/Bi:YIG)^5$/Bi:YIG periodic structure in figure 4(*b*) are depicted. In this case, because of the lack of defect in the periodic structure, no resonant transmission due to the light localization is available. It should be noted, however, that considerable enhancement in Faraday rotation is seen at the band edges of approximately 750 nm (small enhancement) and 1050 nm (large enhancement). This is explained from the phase mismatch compensation of light at the band edges and is discussed in [4, 53] in detail.

1D PCs with ferromagnetic metal films, Co-ferrite films, ferromagnetic granular films, and GaAs:MnAs semiconductor films were also fabricated and discussed (for details see [25–29, 62]). Quite recently, epitaxial-grown film samples were prepared with PLD by Kahl and Grishin [52], the first all-garnet 1D PCs with $Bi_3Fe_5O_{12}$ and $Y_3Fe_5O_{12}$.

3.2. Nonlinear optical and magneto-optical properties

The nonlinear optical and magneto-optical properties of media have also been investigated with the spectroscopic measurement apparatus shown in figure 8. The key feature of magnetophotonic crystals and microcavities is the appearance of the photonic bandgap and resonant microcavity modes. Thus, nonlinear optical studies of these structures must be concentrated on the spectroscopy of the nonlinear optical effects. The latter strongly demands the use of tunable laser systems with a broad tuning range to cover the photonic bandgap spectral intervals and microcavity modes. As shown in figure 8, the nonlinear studies were done with a Spectra-Physics MOPO 710 parametric light oscillator (OPO), tuning in the range of 430 to 1500 nm, with a 4 ns pulse duration and a pulse energy of approximately 10 mJ, excited by the third-harmonic of the output of a YaG:Nd^{+3} laser.

Nonlinear magneto-optical Kerr effect (NOMOKE) in magnetization-induced second-harmonic generation (MSHG) intensity was observed in the magnetophotonic microcavity (figure 4 (*a*)) at wavelengths of the resonant localization modes

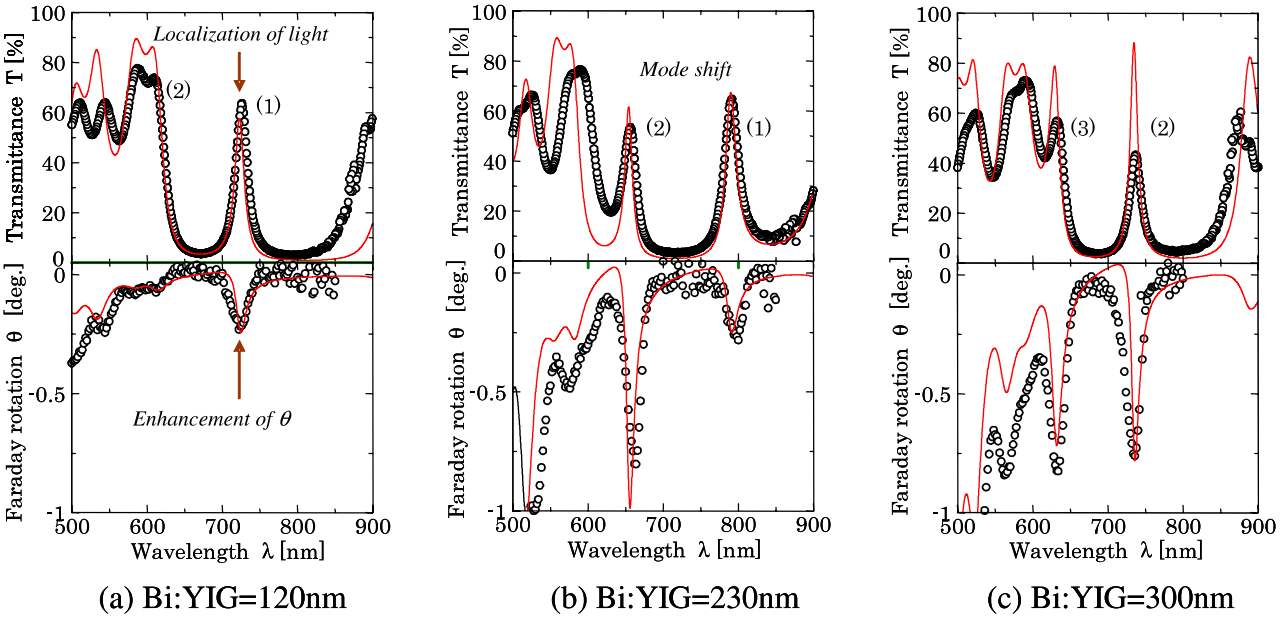

Figure 6. Optical and MO responses of the 1D-magnetophotonic microcavities with three different thicknesses of the central Bi:YIG film, where the solid curves and open marks denote, respectively, the calculated and observed values.

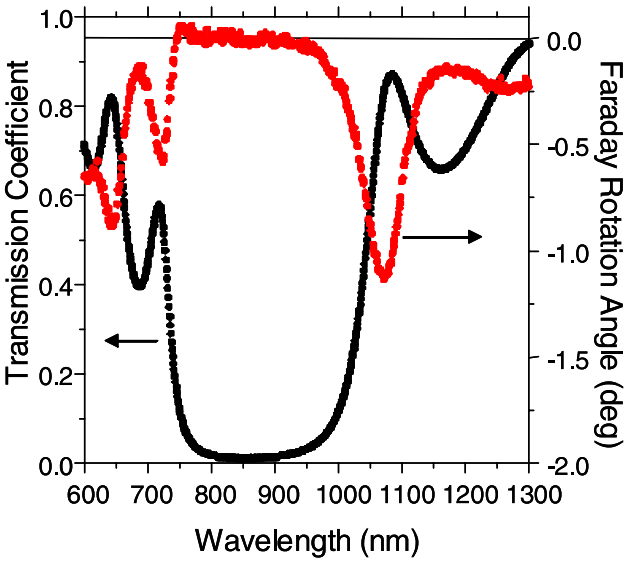

Figure 7. Optical and magneto-optical responses of the 1D-MPC with $(SiO_2/Bi{:}YIG)^5/Bi{:}YIG$ structure shown in figure 4(*b*).

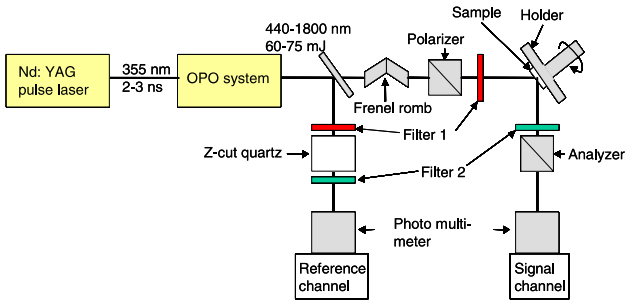

Figure 8. Experimental set-up for the nonlinear studies of MPCs: For frequency domain, fundamental radiation wavelength was tuned at the fixed angle of incidence. The energy and the pulse width were, respectively, about 10 mJ per pulse and below 2 ns, and the spot area was below 0.5 mm^2. For wave-vector domain, the 1064 nm output of a nanosecond YaG laser was used. Energy was below 10 mJ per pulse, pulse width was approximately 15 ns, and the spot area was 1.0 mm^2. External magnetic field of 2 kOe was applied to the sample with a FeNbB magnet.

(figure 9(*a*)) and in the magnetophotonic crystal (figure 4(*b*)) in the spectral range of PBG edges (figure 9(*b*)). In both cases, large enhancement in the MSHG intensity was observed. In the microcavity sample (figure 9(*a*)), significant enhancement of the absolute value of MSHG intensity is attributed to the localization of resonant fundamental radiation in Bi:YIG spacers. When the fundamental wavelength is tuned in the vicinity of the PGB edge, the enhancement factor of MSHG becomes more than 10^2, where as the magnetic contrast reaches almost unity (figure 9(*b*)). This is due to the phase mismatch compensation of light.

Magnetization-induced shift of phase and rotation of polarization of the SH wave were also observed in proper transversal, longitudinal and polar NOMOKE configurations. For instance, figure 10 shows a typical SH-intensity dependence on the orientation of the analyzer axis observed in the microcavity film. This was measured for two opposite directions of saturating magnetic field in longitudinal geometry of NOMOKE. In the figure, the fundamental wavelength corresponds to that of the microcavity mode. The SH wave is strongly linear–polarized, and the application of a field leads only to the rotation of the SH wave polarization. The angle of polarization rotation is 48° for the incidence angle of 15° (figure 10, left), while it is 38° for the 30° incidence (figure 10, right).

Not only MSHG but magnetization-induced third harmonic generation (MTHG) was also studied, where the magnetization-induced intensity variations as well as the magnetization- induced shift of phase and rotation of polarization of SH and TH waves were discussed in detail [7, 53–58].

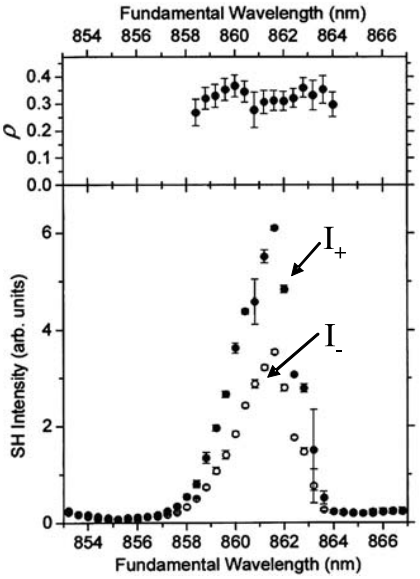

(a) microcavity

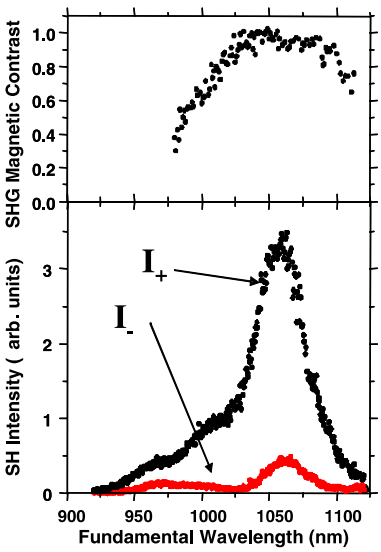

(b) periodic structure

Figure 9. Nonlinear transverse Kerr effect of the localized mode in microcavity structure (*a*) and at the band edge of periodic multilayered film (*b*): Change in SH intensity of light for p-in and p-out configuration (below). I_+ and I_- denote the SH intensities for opposite directions of magnetization. In both cases, corresponding magnetic contrast $\rho = (I_+ - I_-)/(I_+ + I_-)$ is also depicted.

4. 2D and 3D magnetophotonic crystals

The unique feature of magnetophotonic crystals observed in the 1D case implies another potential in media with 2D or 3D spatial symmetry. In fact, Nishizawa *et al* [63] suggested theoretically that, in a 3D magnetophotonic crystal with dielectric ferromagnetic spheres which are placed in fcc lattice, light propagating perpendicularly to the magnetization exhibits a unique magneto-optical effect called a band Faraday effect, which has never been observed in a continuous uniform medium. It was Figotin *et al* [8] who predicted the occurrence of strong spectral asymmetry (non-reciprocity

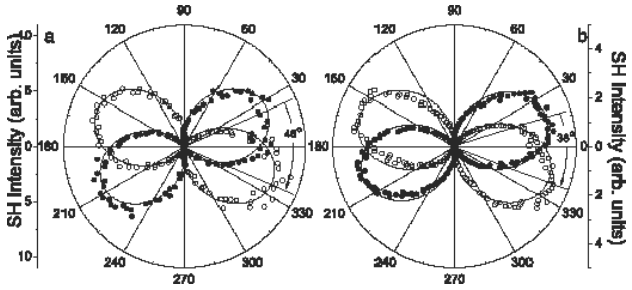

Figure 10. SH polarization diagrams measured for two opposite directions (open and solid marks) of magnetic field applied in the longitudinal configuration. The angles of incidence of s-polarized fundamental radiation were 15° (*a*: left) and 30° (*b*: right). The zero value of the analyzer angle corresponds to the p-polarized SH wave.

or unidirectional propagation of light) in magnetophotonic crystals with a proper spatial arrangement of magnetic and dielectric components. This is also never realized in conventional non-magnetic PCs. Recently, Khanikaev *et al* [64] constructed a solvable 2D model and pointed out theoretically that, if the off-diagonal dielectric element of the assumed magnetic material is one order of magnitude larger than that of an existing material, the degeneracy in the photonic band structure can be removed by the presence of a magnetic field. They also predicted that, despite the small off-diagonal dielectric element ($\varepsilon_{12} \ll \varepsilon_{11}$), a highly sensitive magnetic feature appears in light at the band edges indicating controllability of PBG with a magnetic field. This was also confirmed theoretically with a generalized model [65], where a magnetically controllable super-prism effect was predicted to occur, although their medium structure is ideal, which goes beyond the current micro-process accuracy. Nevertheless, to proceed with the experimental studies on magnetophotonic crystals, our first task seems to be the realization of magnetophotonic crystals with perfect 2D or 3D spatial symmetry.

4.1. Formation of garnet-based 2D magnetophotonic crystals

To form magnetic garnet-based 2D magnetophotonic crystals, several methods have been examined: A typical bottom-up method is the use of self-organized alumina (Al_2O_3) plates with almost perfect periodic pore structures. As Masuda *et al* [66] described, such a medium can be obtained through a self-organized anodization process of Al with shallow trigger pits. In fact, as shown in figure 11(*a*), their technique was effective in obtaining a porous alumina template with considerably good periodic array structures of nano-scaled pores, where the diameter and spacing of pores were approximately 200 nm after the pore-widening post-process. The thickness of the template was controllable with the anodization time ranging from several micrometers to several hundred micrometers.

The alumina template, whose pore diameter and spacing were approximately 60 nm and 100 nm, respectively, was employed in the formation of 2D magnetophotonic crystals as a mask in the physical etching of the Bi:YIG precursor film with an amorphous structure (as-deposited film) [9]. After the etching, the film was subjected to rapid thermal treatment at 700 °C for 10 min. As shown in figure 11(*b*), the alumina pattern was successfully transcribed to the film

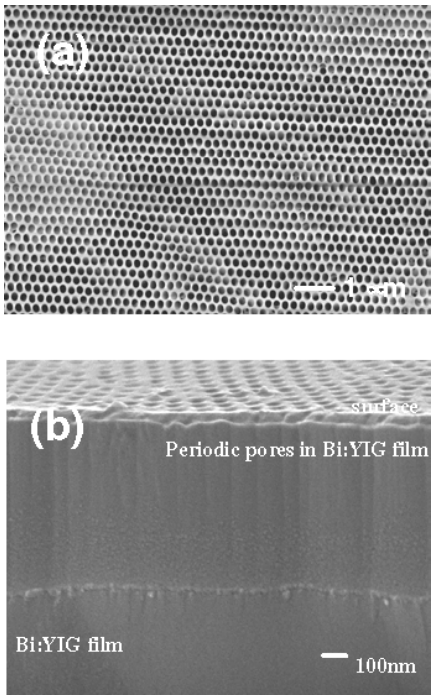

Figure 11. (*a*) a typical porous alumina template (approximately 3 μm thick) formed in oxalic acid solution (0.3 mol L^{-1}) at 10 °C with a constant voltage of 40 V. The pore structure was prepared with an aluminium plate (99.999 purity) with the pre-texture (trigger pits) formed by e-beam lithography. (*b*) 2D magnetophotonic crystal composed of Bi:YIG film with periodic pore structure. The film was prepared by physical etching with the alumina template as a mask.

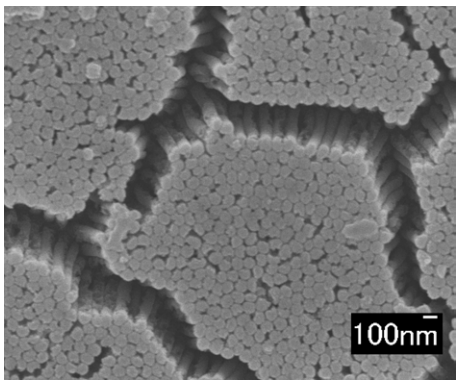

Figure 12. Nano-poles of Bi-substituted YIG (Bi:YIG) which were formed with the porous alumina template and .Bi:YIG precursor sol–gel solution.

and the resultant Bi:YIG film had a 2D periodic hole structure. Unfortunately, however, the thickness of the structured Bi:YIG film was no more than 700 nm, the value of which was inadequate for optical examination. To overcome this, another trial is now under progress, where the alumina template is used as a container of sol–gel Bi:YIG precursor solution (the sol–gel solution was formed in accordance with our previous works in 1998 [67].) as shown in figure 12, this method enables us to form magnetic garnet nano-poles, and is then expected to be a good candidate for realizing 2D magnetophotonic crystals with perfect periodicity (inversion of the pore structure).

Contrary to the bottom-up method, selective-area epitaxial growth of magnetic garnet films has been studied for 2D-MPC formation, Park *et al* [10] deposited garnet films on SGGG (111) substrates at 700 °C with the target of $(Bi_{1.5}Y_{1.5}Gd_{0.2})(Fe_{3.8}Ga_{1.2})O_X$ composition by RF dual ion-beam sputtering. The SGGG surface had pre-patterns with Al_2O_3, SiO_2 or Pt, and the films formed on the masked SGGG surface had non-magnetic amorphous-like structures. Then, by forming an appropriate pattern on the SGGG surface, the resultant garnet film had magnetically discontinuous 2D structures separated by the amorphous-like non-magnetic regions. Typical sample surfaces observed by the polarization microscope are depicted in figure 13 for two spatial periodicities. Refractive indices of the garnet epitaxial film and the amorphous-like film were evaluated to be 2.4 and 2.1, respectively, suggesting a low index contrast between them. Then, to obtain a deep photonic band gap in light (electromagnetic wave) propagations, removal of the amorphous-like separator seems to be necessary. On the contrary, however, the magnetostatically-connected 2D periodic array appears to be attractive in manipulating spin-waves with the nature of the band-gap [68]. In either case, the selective-area epitaxy is one of the useful methods for 2D samples by having the advantage of easy introduction of point or line defects into the periodic structures for supporting the localized modes of waves.

4.2. 3D magnetophotonic crystals

An artificial opal (3D PCs composed of dielectric fine particles with the diameter to each other) [69,70] can be a good template in the formation of 3D magnetophotonic crystals, where magnetically active materials such as magnetite, Bi:YIG, terbium gallium garnet (TGG), terbium aluminium garnet (TaG) are filled up into the free periodic space within the opal [71,72]. To obtain the opal template, we used the vertical deposition method [79–81]: a hydrophilic glass substrate was vertically immersed into a warm colloidal suspension, in which SiO_2 fine particles had been dispersed in water, and the opal was self-organized associated with the evaporation of water. Figure 14 shows SEM images of the SiO_2 opal template thus prepared whose crystallographic structure was identified as ⟨111⟩ oriented fcc from the optical bandgap measurements [82].

3D magnetophotonic crystal was obtained by filling up the opal template with the garnet precursor gel solution composed of $Bi(NO_3)$, $Y(NO_3)$ and $Fe(NO_3)$ which were dissolved in DMF. The desiccated samples were subject to post-annealing at 750 °C for garnet formation. SEM images in figure 15(*a*) show that the sample thus prepared had a composite structure, in which the overall void space of the SiO_2 opal template was filled up with garnet. In fact, as shown in figure 15(*b*), a clear shift in the bandgap appeared associated with the change in void materials from air (in original opal) to garnet. In general, transmissivity of the samples decreases in the visible as a result of light absorption and scattering by magnetic fine particles. Because of this, the relative intensity of the (111) photonic bandgap decreases in comparison with that of the initial opal sample. As a matter of course, the transmission wavelength spectra of samples depend strongly on the volume fraction of magnetic materials embedded into the opal voids. In spite of the small volume fraction of garnet (saturation magnetization

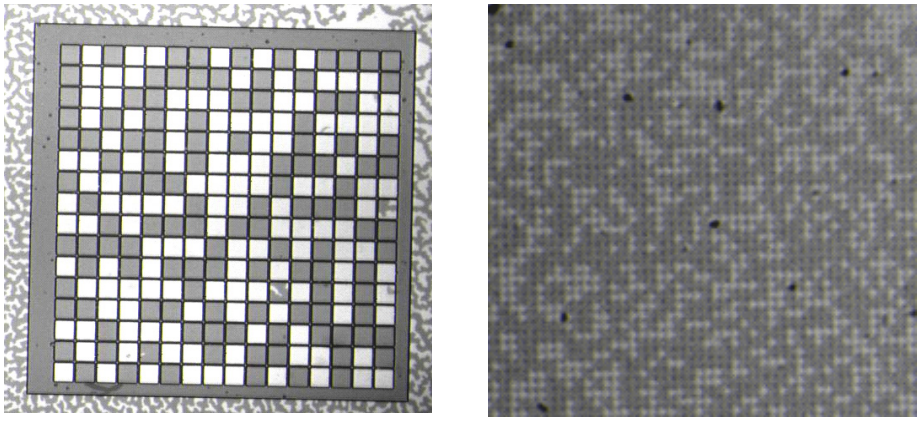

Figure 13. Polarization microscope images of the magnetic garnet films with perpendicular magnetization (approximately 2.8 μm thick) prepared by the selective area epitaxy: 15 × 15 μm^2 garnet squares with 1 μm gap (left) and 0.8 × 0.8 μm^2 garnet squares with 0.8 μm gap (right).

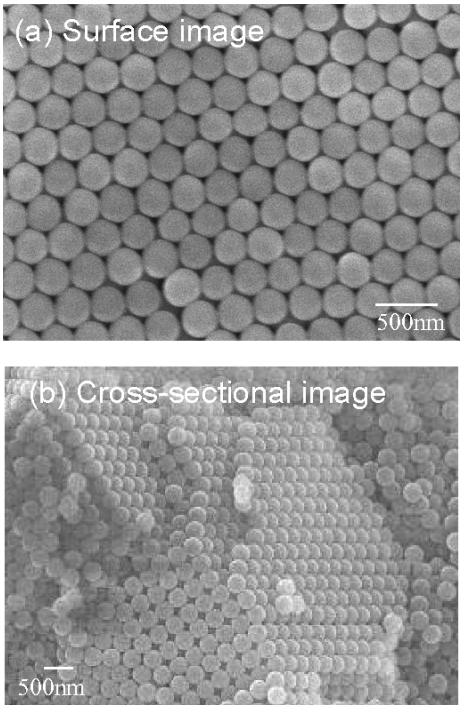

Figure 14. SEM images of the SiO_2 opal template with <111> oriented fcc structure prepared by the vertical deposition method. The diameter of SiO_2 particles was approximately 260 nm.

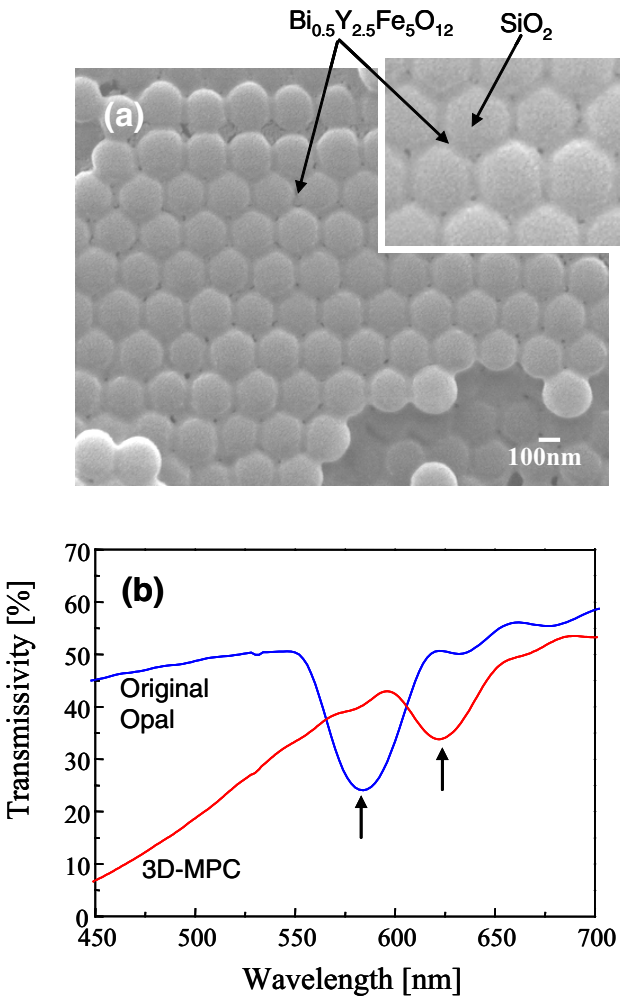

Figure 15. (*a*) SEM images of the SiO_2 opal filled with magnetic garnet ($Bi_{0.5}Y_{2.5}Fe_5O_{12}$). Right corner inset is the magnification. (*b*) Wavelength spectra of the transmissivity of samples.

was 2.5×10^{-4} emu), the sample showed approximately 1.5° Faraday rotation at 525 nm. Unfavourably, however, no clear effect of the bandgap on the magneto-optical spectrum was observed. To explain this, theoretical calculations are now underway.

In terms of the transmissivity in the visible, Verdet materials such as Tb-Ga garnet (TGG) or Tb-Al garnet (TaG) are useful owing to their low optical dissipations, although these paramagnetic materials require a considerably large magnetic field for magneto-optical response. In magnetite-based samples, unique enhancement of the Faraday rotation within the photonic bandgap was observed, contrary to the 1D case where the enhancement was observed at the band edge. This is also confirmed, more clearly, with an opal sample immersed in a transparent paramagnetic liquid [71, 73, 76].

Introduction of magnetic defects into the opal was also examined. The opal template shown in figure 14 has a firm

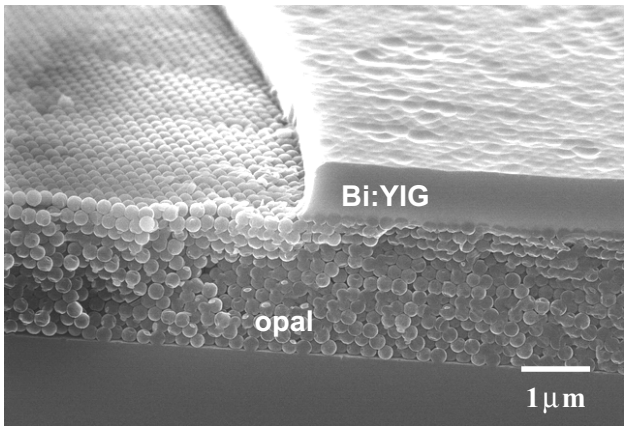

Figure 16. SEM image of a Bi:YIG film which was directly deposited onto the opal template by RF magnetron sputtering.

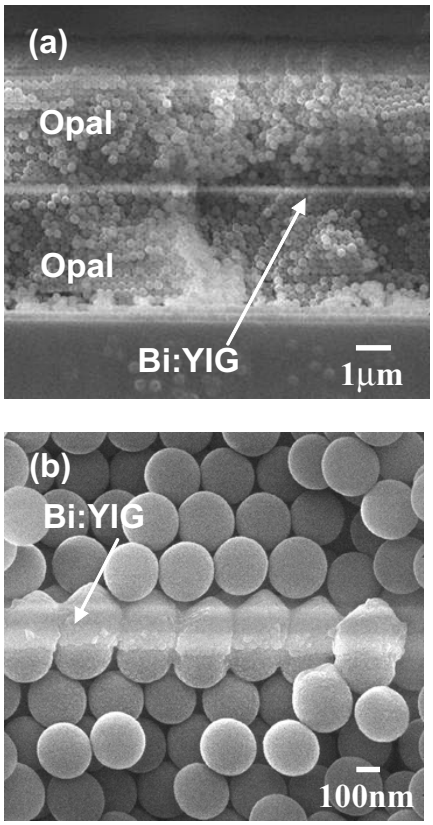

Figure 17. (*a*) Cross-sectional SEM image of the SiO_2 opal with a magnetic (Bi:YIG) plane defect. (*b*) Its magnification.

structure and a flat surface, enabling the formation of Bi:YIG films by sputtering directly onto the top of the template. As shown in figure 16, the surface state of the Bi:YIG film on opal and the interface between the Bi:YIG film and opal are both good even after the post-annealing at 750 °C for garnet crystallization. By using the vertical deposition method, SiO_2 fine particles were self-organized on the Bi:YIG film. Then, as shown in figure 17, a SiO_2 opal containing the Bi:YIG thin film as a plane magnetic defect was obtained. Due to the existence of photonic bandgap and the magnetic plane defect, the sample exhibited unique optical and magneto-optical properties. The details will be reported elsewhere [83].

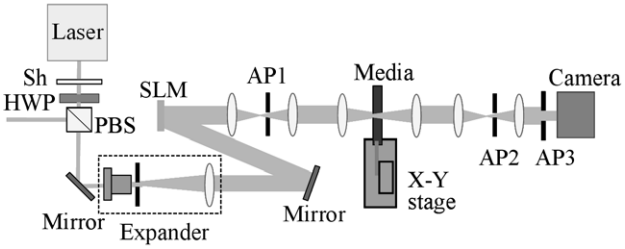

Figure 18. An optical configuration for the transmission-type collinear holography.

5. Applications of magnetophotonic crystals

Owing to their unique linear and nonlinear magneto-optics as well as the spin-dependent nature of bandgap structures, magnetophotonic crystals have already found several electronic applications. In the 1D case, film-type optical isolator/circulator devices have been examined by several authors [19, 30–36]. In fact, the 1D media whose optical and MO properties simultaneously meet the isolator requirements can be designed in combination with dielectric films. According to Kato and Inoue [32], the 1D medium with the structure of $(Ta_2O_5/SiO_2)^8$/Bi:YIG/$(SiO_2/Ta_2O_5)^8$/SiO_2/$(Ta_2O_5/SiO_2)^8$/Bi:YIG/$(SiO_2/Ta_2O_5)^8$ simultaneously exhibits transmissivity $T = 99.99\%$ and Faraday rotation angle $\theta = 44.33°$ at $\lambda = 1.3\,\mu$m for transmitting light through the fillm, while the media with $(SiO_2/Ta_2O_5)^9$/Bi:YIG/$(Ta_2O_5/SiO_2)^{19}$ structure exhibits reflectivity $R = 99.91\%$ and Kerr rotation angle $\theta_K = 44.23°$ at $\lambda = 1.3\,\mu$m for reflected light. In both cases, media thicknesses are considerably thin enabling the formation of film-type isolator devices (total Bi:YIG thickness is t_M=550 nm and total film thickness is $t_A = 12.98\,\mu$m for the former, while $t_M = 275$ nm and $t_A = 19.94\,\mu$m for the latter.) The large MO effects are, however, accompanied by very narrow wavelength spectra due to the localization (resonation), which becomes unfavourable for practical optical communications. A measure to resolve this could be a cascade stacking of films, which is now under examination by actually constructing the film samples.

Magneto-optic spatial light modulators (MOSLMs) are another good application of the 1D magnetophotonic crystals. There are various types of reusable modern SLMs with a 2D array of pixels, which have been intensively developed over the past three decades [6]. Of these, MOSLMs have the advantages of very high switching speed, solid-state and robustness, nonvolatility, and radioactive resistance [27, 38]. Unfavourably, however, the devices developed so far had a serious heat problem in their operations because large drive currents reaching 200 mA were needed to reverse the magnetization in a pixel. Recent renewed interest in MOSLMs has resulted from the development of optical volumetric recording with holography [39,40], particularly, collinear holography [84,85]. As shown in figure 18, collinear holography utilizes the SLM for both writing and retrieving processes, where a high speed SLM is essential for ensuring the high transfer rate. For such a purpose, MOSLM becomes very attractive due to its high operation speed. In fact, the pixel switching speed of approximately 15 ns was reported [86] in MOSLMs with LPE-grown magnetic garnet films [42–50]. In these devices,

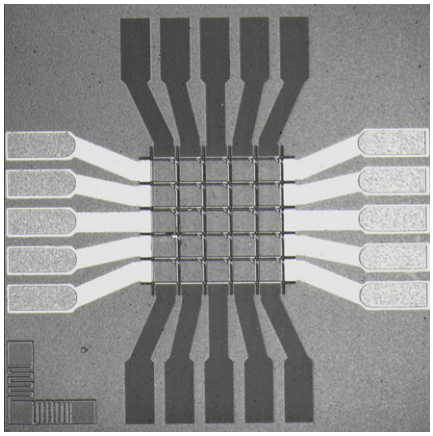

Figure 19. A current-driven MOSLM (5 × 5 pixels) composed of the 1D microcavity with a Bi:YIG film sandwiched between two dielectric Bragg mirror films. The X–Y current lines for driving magnetic pixels were formed with ITO thin film which were inserted between Bi:YIG and dielectric mirror films.

optical efficiency, or magneto-optical contrast of each pixel, can be improved by making use of a thick magnetic garnet film, at the expense of facility in micro-fabrication of the devices. For such requirements, 1D magnetophotonic crystals are useful because they simultaneously exhibit considerably large MO effect and high transmissivity with thin magneto-active layers. In contrast to the case of optical isolator devices, the narrow bandwidth of the resonant transmission of light in the magnetophotonic crystals will not be a serious problem in the holographic data storage, where a highly stable coherent monochromatic light is employed. Figure 19 shows the first current-driven MOSLM with the 1D magnetophotonic microcavity. The performance of this device, as well as that of voltage-driven MOSLM with the 1D magnetophotonic microcavity, will be reported in the near future. Another application of the 1D media can be also found in [51] as MO recording media.

For 2D and 3D media, more sophisticated applications are considered. Recently, Wang *et al* [78] theoretically analysed the performance of a 2D magnetophotonic microcavity and concluded that a planar-type small optical circulator device having high-performance and large bandwidth can be constructed with the 2D media. According to Khanikaev *et al* 64, 65], a magnetically controllable super-prism can be constructed with two- or three-dimensional magnetophotonic crystals when they are operated at the photonic band edges. This effect can be expected to occur in the 1D case, and experimental confirmation is now underway with the 1D media.

6. Conclusion

The unique features of magnetophotonic crystals were reviewed based mainly on our investigations. As far as the 1D case is concerned, almost perfect layered media with dielectric-garnet composites or all garnet structures have been obtained and their properties were studied experimentally and theoretically in detail. Because of their facility in formation, these media have already found their potential applications in optical isolator/circulator devices, spatial light modulators and sensor/imager systems. Recent developments in this area are combined phenomena such as the relation among photonic bandgap, localized modes and the excitation of surface plasmon, or the enhancement of magnetorefractive effect observed in the far infrared [75, 76]. Their experimental investigations have already been started.

The current issue is the formation of magnetophotonic crystals with perfect 2D or 3D spatial symmetries. Several trials have been made, but the results are still unsatisfactory. Because these samples are expected to exhibit unique spin-dependent linear and nonlinear optical properties, though the structures are sometimes very complicated, further vigorous studies for creating the novel media are necessary. Apart from the optics, particular attention should be given to magnetophotonic crystals such as spin-wave media. By utilizing the photonic bandgap or localization, unique manipulation of spin-waves will be feasible. From the engineering points of view, this is attractive for high frequency applications ranging from gigahertz to terrahertz.

In conclusion, magnetophotonic crystals are spin-dependent bandgap materials which will open up new directions in photonics and magneto-optics. To make them materialize and utilize them in practical applications, further fundamental studies are necessary.

Acknowledgments

The authors are grateful to Drs J Akedo and J H Park (AIST), Dr T Dolgova (Moscow State University), Dr J D Joannopoulos (MIT), Drs L Hesselink and S Fan (Stanford University), Dr J K Cho (Kyonang University), Dr H Kato (Minebea Corporation), Mrs H Umezawa and T Imura (FDK Corporation), Dr Y Tanaka (Memory Tech Corporation) and Mr H Horimai (Optware Corporation) for their valuable collaboration and discussions throughout the investigations. The authors also express their sincere appreciation to Dr T Fujii for his continuous, instructive suggestions.

The work was supported in part by the Super Optical Information Memory Project from the Ministry of Education, Culture, Sports, Science and Technology of Japan (MEXT), and Grant-in-Aid for Scientific Research (S) No. 17106004 from Japan Society for the Promotion of Science (JSPS). Development of the Analog-MOSLMs has been supported in part by the NEDO Nano Technology Program, Nano Structure Forming for advanced Ceramic Integration Technology in Japan.

References

[1] Joannopoulos J D, Meade R and Winn J 1995 *Photonic Crystals* (Princeton NJ: Princeton University Press)
Fujii T and Inoue M 2000 *Photonic Kessho* (Tokyo: Corona) (in Japanese)
[2] Inoue M, *et al* 1999 *Proc. 2nd Int. Symp. on Frontiers in Magnetism (Stockholm, August 1999)*
[3] Takayama T *et al* 2000 *J. Magn. Soc. Japan.* **24** 391 (in Japanese)
[4] Fedyanin A A, *et al* 2004 *IEEE Trans. Magn.* **40** 2850
[5] Kato H, *et al* 2002 *IEEE Trans. Magn.* **38** 3246
[6] Park H J, Nishimura K, Cho J K and Inoue M 2002 *J. Magn. Soc. Japan.* **26** 729 (in Japanese)

[7] Aktsipetrov O *et al* 2004 *Laser Phys.* **14** 685
Aktsipetrov O *et al* 2005 *J. Opt. Soc. Am.* B **22** 176
[8] Figotin A and Vitebsky I 2001 *Phys. Rev. E* **63** 066609
[9] Ikezawa Y, Nishimura K, Uchida H and Inoue M 2004 *J. Magn. Magn. Mat.* **272–276** 1690
[10] Park J K, Nishimura K, Uchida H and Inoue M 2005 *Intermag 2005 Conf. (Nagoya, Japan)* abstracts
[11] Merzlikin A M, Vinoradov A P, Inoue M and Granovsky A B 2005 *Phys. Rev.* E **72** 046603
[12] Baryshev A, Kodama T, Nishimura K, Uchida H and Inoue M 2004 *J. Appl. Phys.* **95** 7336
[13] Inoue M, Isamoto K, Yamamoto T and Fujii T 1996 *J. Appl. Phys.* **79** 1611
[14] Inoue M and Fujii T 1997 *J. Appl. Phys*. **81** 5659
[15] Inoue M, Fujii T, Arai K I and Abe M 1998 *J. Magn. Soc. Japan.* **22** 141
[16] Inoue M, Arai K I, Fujii T and Abe M 1998 *J. Magn. Soc. Japan.* **22** 321 (in Japanese)
[17] Inoue M and Fujii T 1997 *J. Magn. Soc. Japan.* **21** 187 (in Japanese)
[18] Inoue M and Fujii T 1999 *Papers of Tech Meeting on Magn. IEE Japan* MaG-99-168 (Tokyo: IEE Japan) (in Japanese)
[19] Steel M J, Levy M and Osgood R M Jr. 2000 *J. Lightwave Technol.* **18** 1297
[20] Inoue M, Arai K I, Fujii T and Abe M 1998 *J. Appl. Phys.* **83** 6768
[21] Inoue M *et al* 1999 *J. Magn. Soc. Japan.* **23** 1861 in Japanese
[22] Vinogradov A P, Erokhin S G, Granovsky A B and Inoue M 2004 *J. Commun. Technol. Electron.* **9** 88
[23] Vinogradov A P, Erokhin S G, Granovsky A B and Inoue M 2004 *J. Commun. Technol. Electron.* **9** 682
[24] Inoue M, Arai K I, Fujii T and Abe M 1999 *J. Appl. Phys.* **85** 5768
[25] Inoue M, Matsumoto K, Arai K I, Fujii T and Abe M 1999 *J. Magn. Magn. Mater.* **196–197** 611
[26] Inoue M, Arai K I, Fujii T and Abe M 2000 *Korean J. Ceramics* **6** 408
[27] Takeda E *et al* 2000 *J. Appl. Phys.* **87** 6782
[28] Abe M *et al* 2000 *Korean J. Ceramics* **6** 100
[29] Yoshida T, Nishimura K, Uchida H and Inoue M 2003 *J. Appl. Phys.* **93** 6942
[30] Sakaguchi S and Sugimoto N 1999 *J. Lightwave. Technol.* **17** 1087
[31] Kato H, Matsushita T and Inoue M 2002 *J. Magn. Soc. Japan.* **26** 340 (in Japanese)
[32] Kato H and Inoue M 2002 *J. Appl. Phys.* **91** 7017
[33] Kato H *et al* 2003 *Opt. Commun.* **219** 271
[34] Kato H, *et al* 2003 *J. Appl. Phys.* **93** 3906
[35] Kato H *et al* 2004 *J. Magn. Magn. Mater.* **272–276** e1327
[36] Kato H *et al* 2004 *J. Magn. Magn. Mater.* **272–276** e1305
[37] Ross W E, Psaltis D and Anderson R H 1983 *Opt. Eng.* **22** 485
[38] Cho J *et al* 1994 *J. Appl. Phys.* **76** 1910
[39] Coufal H J, Psaltis D and Sincerbox G T (ed) 2000 *Holographic Data Storage (Springer Series in Optical Sciences)* (Berlin: Springer)
[40] Inoue M and Hesselink L 2003 *J. Magn. Soc. Japan.* **27** 635 (in Japanese)
[41] Lisa Dhar 2002 *Proc. 6th Optware Meeting (Tokyo, March 2002)*
[42] Park J H, Cho J K, Nishimura K and Inoue M 2002 *Japan. J. Appl. Phys.* **41** 1813
[43] Park J H, Lee D H, Cho J K, Nishimura K and Inoue M 2002 *J. Appl. Phys.* **91** 7014
[44] Park J H *et al* 2003 *J. Appl. Phys.* **93** 8522
[45] Park J H *et al* 2003 *IEEE Trans. Magn.* **39** 3169
[46] Park J H *et al* 2004 *J. Magn. Magn. Mater*. **272–276** 2260
[47] Park J H *et al* 2003 *J. Appl. Phys.* **93** 8525
[48] Takagi H *et al* 2004 *Mater. Res. Soc. Symp. Proc. (Boston, MA)* vol 785, D610.1
[49] Park J H, Cho J K, Nishimura K, Uchida H and Inoue M 2004 *Japan. J. Appl. Phys.* **43** 4777
[50] Park J H, Takagi H, Cho J K, Uchida H and Inoue M 2004 *IEEE Trans. Magn.* **40** 3045
[51] Inoue M, Arai K I, Fujii T, Abe M and Matsumoto K 2002 Multilayer resonance device and magneto-optical recording mediumwith magnetic center layer of a different thickness than that ofthe components of the reflecting layers and method of reproducingthe same *US Patent* 6,421,303 B1
[52] Kahl S and Grishin A M 2004 *Appl. Phys. Lett.* **84** 1438
[53] Fedyanin A A, Aktsipetrov O A, Kobayashi D, Nishiman K, Uchida H and Inoue M 2004 *J. Magn. Magn. Mater.* **282** 256
[54] Fedyanin A *et al* 2002 *J. Exp. Theor. Phys. Lett.* **76** 527
[55] Fedyanin A *et al* 2003 *J. Magn. Magn. Mater.* **258–259** 96
[56] Murzina T *et al* 2003 *JETP Lett.* **77** 639
[57] Dolgova T *et al* 2004 *J. Appl. Phys.* **95** 7330
[58] Murzina T *et al* 2004 *Phys. Rev.* B **70** 012407-1
[59] van albada M P and Lagendijk A 1985 *Phys. Rev. Lett.* **55** 2692
[60] Wolf P E and Maret G 1985 *Phys. Rev. Lett.* **55** 2696
[61] Gomi M, Saito M and Abe M 1983 *J. Magn. Soc. Japan.* **7** 131 (in Japanese)
[62] Shimizu H, Miyamura M and Tanaka M 2001 *Appl. Phys. Lett.* **78** 1523
[63] Nishizawa H and Nakayama T 1997 *J. Phys. Soc. Japan.* **66** 613
[64] Khanikaev A, Baryshev A, Inoue M, Granovsky A and Vinogradov A 2005 *Phys. Rev.* B **72** 035123
[65] Khanikaev A B, Inoue M and Granovsky A B 2006 *J. Magn. Magn. Mater.* at press
[66] Masuda H *et al* 1997 *Appl. Phys. Lett.* **71** 2771
[67] Fujii T, Nanpei S, Inoue M and Arai K I 1998 *J. Magn. Soc. Japan.* **22** 200 (in Japanese)
[68] Nikitov S, Filimonov Y, Gulyaev Y, Tailhades P and Tsai C 2004 *Abstract Mater. Res. Soc. Fall Meeting (Boston, MA)* J2.2
[69] Astratov V N *et al* 1995 *Nuovo Cimento* D **17** 1349
[70] Vlasov Yu A *et al* 1997 *Phys. Rev.* B **55** R13357
[71] Baryshev A, Kodama T, Nishimura K, Uchida H and Inoue M 2004 *IEEE Trans. Magn.* **40** 2829
[72] Nishimura K, Kodama T, Baryshev A, Uchida H and Inoue M 2004 *J. Appl. Phys*. **95** 6633
[73] Baryshev A, Kodama T, Nishimura K, Uchida H and Inoue M 2005 *Intermag 2005 Conf. (Nagoya, Japan)* abstracts
[74] Granovsky A, Inoue M, Clerc J and Yurasov A 2004 *Phys. Solid State* **46** 498
[75] Boriskina Ju V, Erokhin S G, Granovsky A B, Vinogradov A P and Inoue M 2006 *Phys. Solid State* **4** at press
[76] Koerdt C, Rikken G L J A and Petrov E P 2003 *Appl. Phys. Lett*. **82** 1538
[77] Rosenberg R, Rubinstein C B and Herriott D R 1964 *Appl. Optics* **3** 1079
[78] Wand Z and Fan S 2005 *Appl. Phys.* B **81** 369
[79] Dimitrov A S and Nagayama K 1996 *Langmuir* **12** 1303
[80] Jiang P, Bertone J F, Hwang K S and Colvin V L 1999 *Chem. Mater.* **11** 2132
[81] Zuocheng Zhou and Zhao X S 2004 *Langmuir* **20** 1524
[82] Fujikawa R, Okubo T, Baryshev A, Uchida H, Lim P B and Inoue M 2005 *Tech. Rep. Inst. Electr. Eng. Japan*. **MaG-05-139** (in Japanese)
[83] Fujikawa R, Okubo T, Baryshev A, Uchida H, Lim P B and Inoue M 2006 *J. Magn. Magn. Mater.* at press
[84] Horimai H and Li Jun 2004 *Proc. SPIE* **5380** 297
[85] Lim P B, Kashiwagi K, Oota M, Imura T, Umezawa H and Inoue M 2005 *Tech. Rep. Inst. Electr. Eng. Japan*. **MaG-05-173** (in Japanese)
[86] Inoue M, Iwasaki K, Yamanaka T, Imura T, Umezawa H, Lim B P and Horimai H 2005 *Tech. Rep. Inst. Electr. Eng. Japan*. **MaG-05-184** (in Japanese)